ANALYSIS OF ATTENUATION DATA FROM THE DECOMMISSIONED ZION UNIT 1 REACTOR PRESSURE VESSEL BELTLINE WELD

Mikhail A. Sokolov[1] and Roger Stoller[2]

[1]Oak Ridge National Laboratory

[2]Stoller Materials Consulting

OAK RIDGE NATIONAL LABORATORY
Oak Ridge, TN 37831-6283
managed by
UT-BATTELLE LLC
for the
US DEPARTMENT OF ENERGY
under contract DE-AC05-00OR22725

As submitted – 17 Oct. 2025

Analysis of Attenuation Data from the Decommissioned Zion Unit 1 Reactor Pressure Vessel Beltline Weld

Mikhail A. Sokolov[1] and Roger E. Stoller[2]

[1]Materials Science and Technology Division, Oak Ridge National Laboratory, Oak Ridge TN USA

[2]Stoller Materials Consulting, Knoxville, TN USA

ABSTRACT

In order to examine the attenuation of radiation damage through the thickness of an irradiated reactor pressure vessel (RPV), four segments were acquired from the Zion Unit 1 power plant RPV after the plant was decommissioned. The Zion Unit 1 RPV Beltline Weld Segment 1 was cut into seven blocks, consisting of five base metal and two beltline welds from the high fluence region of the segment. Through-wall test specimens were machined and tested. Specimens included those used for Charpy impact, Master Curve fracture toughness testing, and chemical analysis. The observed through-thickness ductile-to-brittle transition temperatures in the beltline weld deviated significantly from the expected behavior based on the attenuation of fast fluence as a function of depth into the RPV. Beginning at the inside surface, the 41-J Charpy transition temperature was either flat or slightly increasing until the ¾ -T location. The results of a simple, model-based analysis of the Zion beltline weld material that included the irradiation conditions and material chemistry were generally consistent with industry trend curves and the standard attenuation model, rather than the observed data. Although there was no archive material from the RPV available to permit measurement of the unirradiated properties, fracture toughness specimens fabricated from archive surveillance weld were used to obtain an estimate of the initial through-thickness values of the Charpy transition temperature. The Charpy shifts obtained using this approach were similarly in disagreement with the predictions of the US NRC Regulatory Guide 1.99, Rev. 2. However, testing of irradiated Charpy specimens taken from the RPV following post-irradiation annealing (10 hr. at 500°C) provided a quite different estimate of the unirradiated properties which improved the agreement between the inferred through-thickness Charpy shifts and exponential attenuation model included in Regulatory Guide 1.99/2. The analysis of the Zion data and data obtained in previous post-mortem examinations of decommissioned RPVs indicates that more work is needed to understand the through-thickness properties of RPV materials in order to properly assess through-wall damage attenuation.

Keywords: reactor pressure vessel, irradiation effects, mechanical properties, damage attenuation, Charpy impact, Master Curve fracture toughness

INTRODUCTION

The Zion Nuclear Generating Station in Zion, Illinois consisted of two Westinghouse 4-loop pressurized water reactors, with each unit capable of producing 1,040 MWe. The units were commissioned in 1973, permanently shut down in 1998, and placed into SAFSTOR (a method of decommissioning where a nuclear facility is placed and maintained in a condition that allows the facility to be safely stored and subsequently decontaminated to levels that permit release for unrestricted use) in 2010. The decommissioning of these reactors presented a unique opportunity for developing a better understanding of materials degradation and other issues associated with extending the lifetime of existing nuclear power plants (NPPs) beyond 60 years of service. To support the current operation and extended service of the US nuclear reactor fleet, the Oak Ridge National Laboratory (ORNL) procured components from the decommissioned reactors, including multiple segments of the Zion Unit 1 Reactor Pressure Vessel (RPV). The effort was supported by the Department of Energy (DOE) Light Water Reactor Sustainability (LWRS) Program Long-Term Performance Pathway, and coordinated with Zion Solutions, LLC, a subsidiary of Energy Solutions (ES).

The Zion Unit 1 RPV was composed of a removable hemispherical top head, three ring or shell sections comprising semi-cylindrical plates with two vertical welds, and a hemispherical bottom head. The total height of the RPV without the top head plate was approximately 419 inches (1,064 cm). The vessel wall had an inner diameter of 173 inches (439 cm) and a thickness of 8.8 inches (22.4 cm) over the beltline region. The nozzle ring section is approximately 11 inches thick. Including cladding, the reactor vessel weighed about 700,000 lbs. (317,515 kg).

The Zion Unit 1 RPV was cut using an oxy-propylene torch into 17 segments over four levels. The Zion Unit 1 Beltline Weld Segment 1, with dimensions of ~ 157.5” x 72.9” x 8.8” (400cm x 185cm x 22cm) and containing the well-characterized WF-70 beltline weld and the base metal A533B heat B7835-1, was cut from just below the circumferential weld between the nozzle section and the intermediate shell. At the Energy Solutions Memphis Processing Facility (MPF), Segment 1 was cut into several blocks Including a total of 5 blocks with base metal and two blocks of weld metal. Details of harvesting efforts from the decommissioned Zion Unit 1 can be found in Ref. [1]. Those blocks were sent to BWXT, Lynchburg VA, for specimen machining [2].

Assessments of the attenuation effects were made using weld metal data, for which the maximum fast flux and fluence at the inside surface were about 1.70×10^{14} n/m^2/s and 7.5×10^{22} n/m^2 (E>1.0 MeV), respectively. The base metal data revealed a strong “surface” effect of the through-thickness distribution of the mechanical properties. It is well known that the ductile-to-brittle transition temperature is lower at the surface layers of thick RPV plates, see [3] for example, than in the middle of the plate. The Zion base

metal Charpy T_{41J} and fracture toughness T_0 transition temperatures through-thickness distribution confirmed that this effect continued to appear after irradiation as well.

BRIEF REVIEW OF THROUGH-THICKNESS CHARACTERIZATION OF DECOMISSIONED RPVs

The RPVs from several decommissioned power reactors have been sampled to examine mechanical property variations through the RPV thickness, and a few special-purpose test reactor experiments have been carried out to obtain insight into this same subject. The major studies are listed in Tables 1 and 2. These previous studies have demonstrated the difficulty of obtaining an unambiguous description of how the properties evolve in a thick section of steel under irradiation, particularly in the case of post-mortem examination of a decommissioned RPV. As reflected in the accepted embrittlement trend curves [4,5], radiation-induced embrittlement is known to be sensitive to a range of material and irradiation parameters, including neutron flux and fluence, irradiation temperature, alloy composition (including minor or "tramp" elements), and product form. Since the change of properties after irradiation is of interest, the unirradiated properties also need to be characterized as a function of location in the vessel. For example, the local alloy chemistry needs to be known as a function of depth in both irradiated and unirradiated materials. Although the average chemistry of the welding rods used to fabricate an RPV may be known, the local chemistry within a fabricated weld cannot be measured prior to irradiation and the unirradiated material will at best be similar to that of the in-service component.

Table 1. Previously decommissioned power reactor RPV studies

Reactor	Country	Type	Shut down	Testing
JPDR	Japan	BWR	1976	1994-1999
Gundremmingen, Unit A	Germany	BWR	1977	~1988-1992
BR-3	Belgium	PWR	1987	1995-1999
Novo-Voronezh Unit 1	Russia	VVER	1984	1993-2000
Chooz-A	France	PWR	1991	1995-1999
Greifswald Unit 1	Germany	VVER	1990	2004-2012
Greifswald Unit 2	Germany	VVER	1990	2004-2012
Greifswald Unit 3	Germany	VVER	1990	2004-2012
Greifswald Unit 4	Germany	VVER	1990	2004-2012
Trawsfynydd	UK	Magnox	1991	1996-2002
Barsebäck 2	Sweden	BWR	2005	2019-2022

Table 2. Damage Attenuation Experiments.

Experiment title	Country	Approximate timeframe
IRL (T~60°C)	USA	early 1970s
ORR Pool Side Facility	USA	late 1970s
IAEA-NRI	Czech Republic	about 2002-2010

Reviews of the major studies listed in Tables 1 and 2 can be found in Refs. [6-7], and references therein. Although in some cases the measured attenuation of embrittlement was generally consistent with the predictions of the attenuation model in the U.S. Regulatory Guide 1.99, Rev. 2 [4], much of the experimental data were confounded by unquantified (and unexpected) variations in both the unirradiated and irradiated mechanical properties. This is well illustrated by a statement quoted from the abstract of Ref. [7], "... issues associated with knowledge of the start-of-life properties throughout the vessel wall sample and material property data scatter have made past measurements non-definitive in establishing attenuation changes." The variation in unirradiated properties has been well documented in data obtained from a detailed through-thickness characterization of a beltline weld cut from the Midland RPV [8]. The importance of this example is that it is the same WF-70 weld that was used in Zion Unit 1 beltline weld. As shown in Fig. 1a, the unirradiated Charpy T_{41J} transition temperature varied by more than 40°C depending on the depth and which section of the weld was tested. Somewhat more modest variations were observed in the international testing program of an A533 grade B class 1 plate prepared for the IAEA and designated as the JRQ reference plate [9] shown in Fig. 1b. The gradient in the toughness near the 1/4-T location contributes to the data scatter of almost 40°C in T_{41J}. Interpretation of the post-mortem attenuation studies of the Gundremmingen Unit A RPV was confounded by similar variability in the unniradiated properties as shown in Fig. 2 [10].

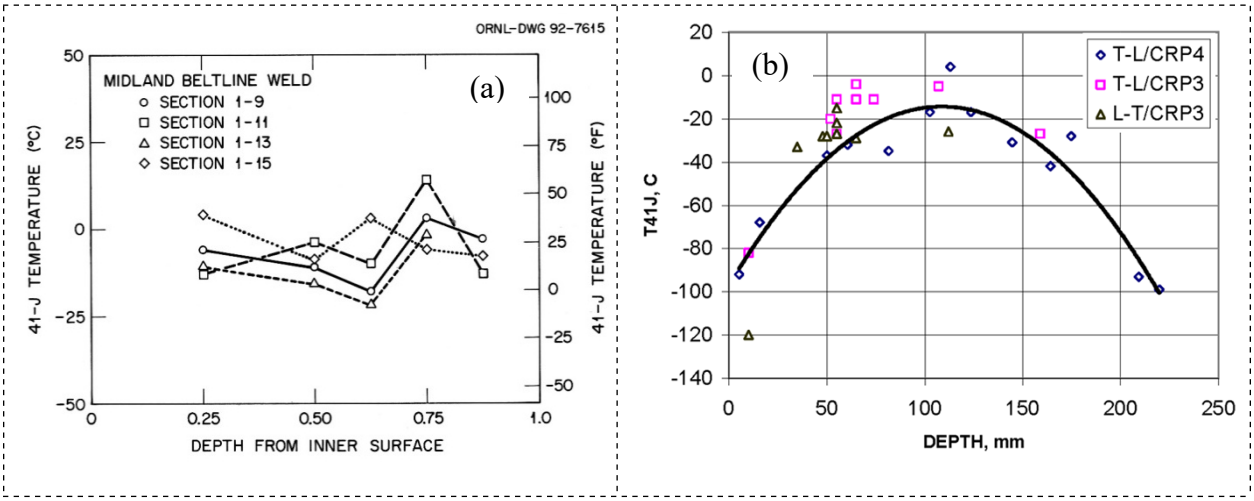

Figure 1. Through-thickness variation in 41J Charpy impact tests for: (a) the Midland beltline weld and (b) JRQ reference plate in unirradiated condition [8, 9].

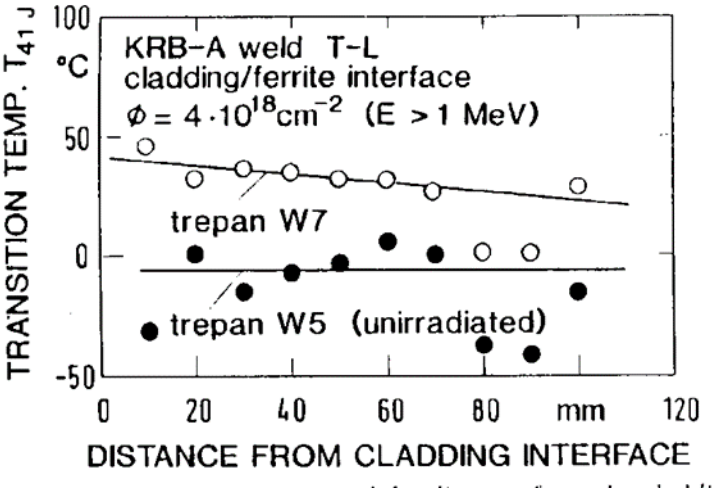

Figure 2. Through-thickness 41J Charpy impact results for the Gundermmingen Unit A weld in the unirradiated and irradiated conditions [10].

The attenuation experiments listed in Table 2 should have provided better opportunities for characterization of the unirradiated materials and control of the experimental variables. However, the results were not as definitive as hoped. As discussed in Ref. [6], the data were similarly confounded by unexpected behavior, which was attributed to experimental uncertainties, unexplained sensitivities to alloy chemistry and Charpy specimen orientation. Even in the most recent experiment, there was evidence of what has been referred to as "anomalous results" [11]. For example, although the master curve data for the JRQ plate material irradiated in the IAEA-NRI experiment shown in Fig. 3 is generally consistent with the dpa-based attenuation model in ASTM E900, it exhibits higher than expected shifts in the 0.3 to 0.5T region and an anomalously high shift at about 0.25-T, where T was the simulated thickness of the vessel wall. In contrast, the Linde 80 weld material included in this experiment exhibited a monotonic and higher rate of embrittlement attenuation, generally exceeding the predictions of the E900 prediction [11].

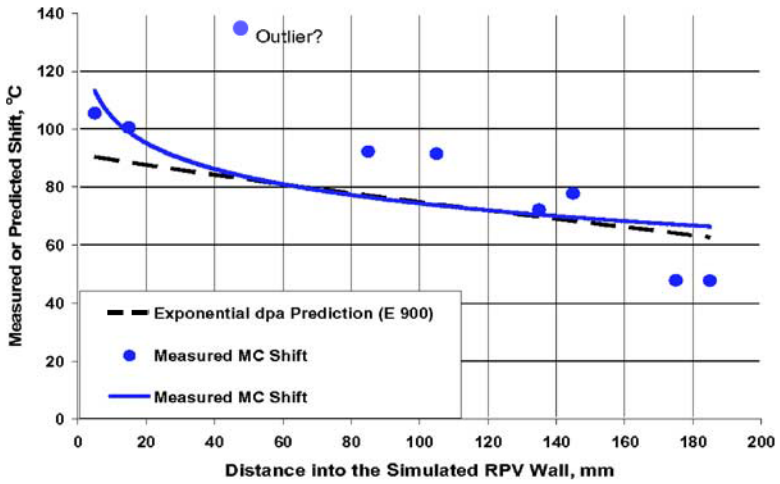

Figure 3. Predicted and measured values of Master Curve T_0 shift for the JRQ plate material [11].

Considering the data shown in Figs. 1-3, and other difficulties discussed in Ref. [6-11], it perhaps is not surprising that understanding the results of the current investigation of the radiation-induced changes in Zion RPV has been a somewhat lengthy process. Some additional comparisons of the Zion data and the previous data will be presented in the section below.

THROUGH-THICKNESS MECHANICAL PROPERTIES DISTRIBUTION OF ZION WELD METAL

For weld metal, all specimens were cut from one block of beltline weld, CF. Fig. 4 shows a schematic cutting diagram of this block presenting the layers with various types of specimens. In the case of weld block CF, layers of Charpy blanks and 0.4T C(T) were alternated through the thickness of the weld. The weld had a V-shape profile with the narrowest portion being the closest to the inner surface of the vessel facing the reactor core. Each layer of Charpy specimens contained 22 Charpy blanks. The first and the last blanks of each layer were used to machine microstructural coupons and tensile specimens. Thus, 20 Charpy specimens were available from each layer for impact testing

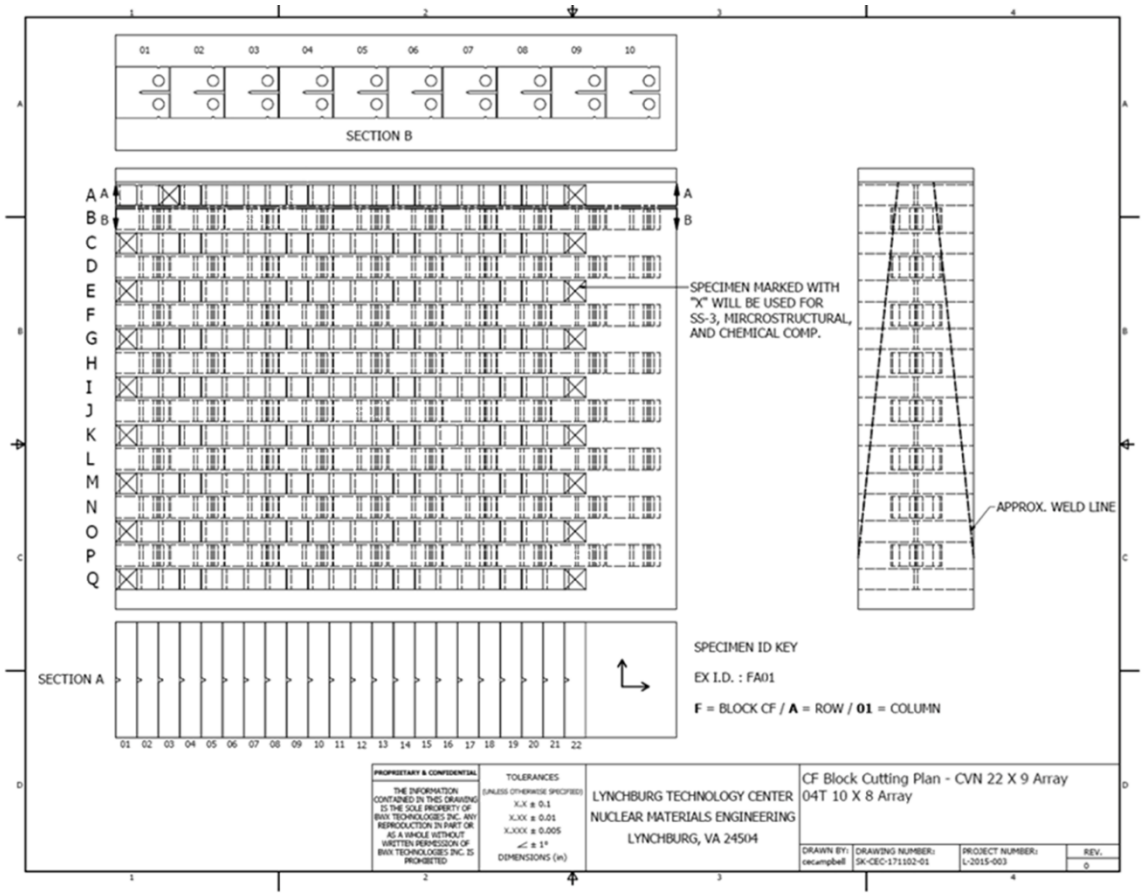

Figure 4. Block CF cutting plan showing alternating layers of Charpy and 0.4T C(T) specimens through the thickness of the vessel [2].

Fig. 5 provides the distribution of the Zion beltline weld Charpy transition temperature, T_{41J}, through the thickness of the vessel wall. It is clear that the values of T_{41J} do not significantly decline through the thickness of the wall until the very last layer. Moreover, the data at about 0.3-T which is designated as "G" in Fig. 4, showed the highest T_{41J} temperature. This behavior is not consistent with the expectation that attenuation of the neutron fluence through the thickness of the vessel should reduce the radiation-induced embrittlement. However, the property of interest when investigating damage attenuation is the change in Charpy transition temperature, ΔT_{41J}, which makes it necessary to determine a best estimate for the unirradiated T_{41J}.

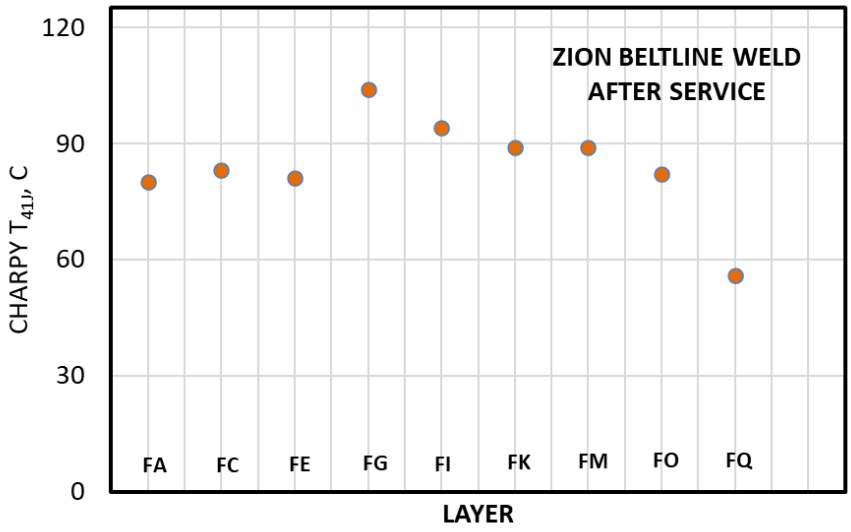

Figure 5. Distribution of the Charpy 41J transition temperature in Zion beltline weld specimens after service.

Assessment of the through-thickness variation of Zion WF-70 beltline weld T_{41J} in the unirradiated condition presented a few challenges. First, there was no proper archive material for the vessel weld itself. Moreover, based on the non-systematic variation of T_{41J} transition temperature of Midland WF-70 beltline weld [8] illustrated in Fig. 1a, it appears that even the use of an archive weld might be problematic. There was an archive weld fabricated for the material used to machine surveillance specimens for Zion Unit 1 RPV. However, this weld is not a WF-70 Linde 80 weld as used in Zion RPV beltline weld. It is WF-209-1 Linde 80 weld. Both welds were made with the same wire and went through the same post-weld heat treatment. The only difference was the lot of welding flux. This should not prevent the use of the WF-209-1 surveillance weld to monitor embrittlement of the RPV beltline weld within the surveillance program, since the chemistry of the weld wire is the leading factor to determine the radiation-induced embrittlement. However, the difference in welding flux lot could potentially introduce a small discrepancy in the absolute value of T_{41J} in the unirradiated condition. Moreover, the Midland beltline study [8] showed that T_{41J} of the beltline weld varied non-systematically even within a single layer (i.e. at a single depth) of the vessel weld.

However, to provide an initial estimate of the RPV weld's unirradiated properties, fracture toughness specimens fabricated from the surveillance weld archive were used. The fracture toughness variation through the vessel thickness was obtained. The results are shown in Fig. 6, where the toughness smoothly and slowly changes through the thickness. Since it is well accepted that Charpy and fracture

toughness transition temperatures are well correlated, the through-thickness dependence of T_0 was used to calculate the through-thickness distribution of Charpy T_{41J} transition temperature in the unirradiated condition. The reported T_{41J} value for the surveillance weld at the ¼-thickess position of the weld was used as a reference point. As shown in Fig. 7, the Charpy shifts obtained using this approach were similarly in disagreement with expectations. There was little change in ΔT_{41J} initially and then a peak at about 0.3T and no significant reduction in embritllement until >0.6T.

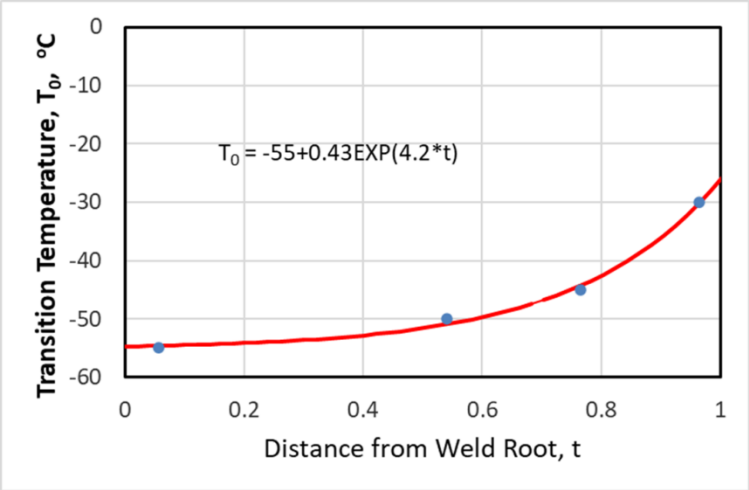

Figure 6. Through-thickness distribution of T_0 in the unirradiated archive surveillance weld.

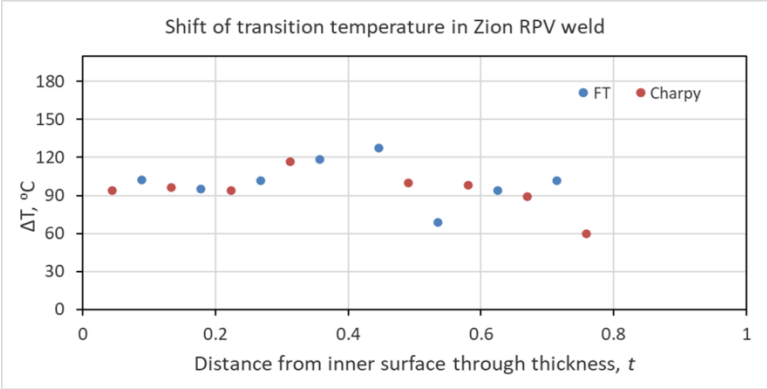

Figure 7. Estimated shift of the fracture toughness (blue) and Charpy 41J (red) transition temperature through the thickness of Zion RPV beltline weld.

The data shown in Fig. 7 are similar in this respect to some data from the IAEA-Czech NRI attenuation experiment [11] which will be discussed below in which there appeared to be little attenuation in the near-surface region. This was followed by an increase in the ΔT_0 at about the 0.25-T depth with

reasonable attenuation behavior at deeper depths. The seemingly random through-thickness distribution of T_{41J} in the unirradiated WF-70 Midland beltline weld (the same weld as the Zion beltline weld) presented in Fig. 1a indicates the need for a better assessment of the through-thickness distribution of T_{41J} of the Zion beltline weld in the unirradiated condition.

Therefore, the through-thickness behavior of the Zion PRV beltline weld was further investigated by annealing irradiated specimens taken from the RPV. As is shown in Fig. 4, each layer of Charpy specimens contained 20 specimens. Only 12 or 13 specimens were used to generate the Charpy transition curves to determine the T_{41J} values presented on Fig. 5. The remaining specimens from layers FA, FC, FG, FI, FK, FO, and FQ were annealed for 10 hr. at 500°C, a treatment that should lead to complete recovery of the radiation-induced property changes [13]. The resulting Charpy T_{41J} data for the annealed Zion beltline weld specimens are presented in Fig. 8. As in the case of Midland weld, the values of T_{41J} for the annealed Zion beltline weld specimens varies through the thickness of the vessel. However, the absolute magnitude of the variation is in general agreement with the Midland data as shown in Fig. 9, where we superimposed the Zion annealed data on Fig. 1.

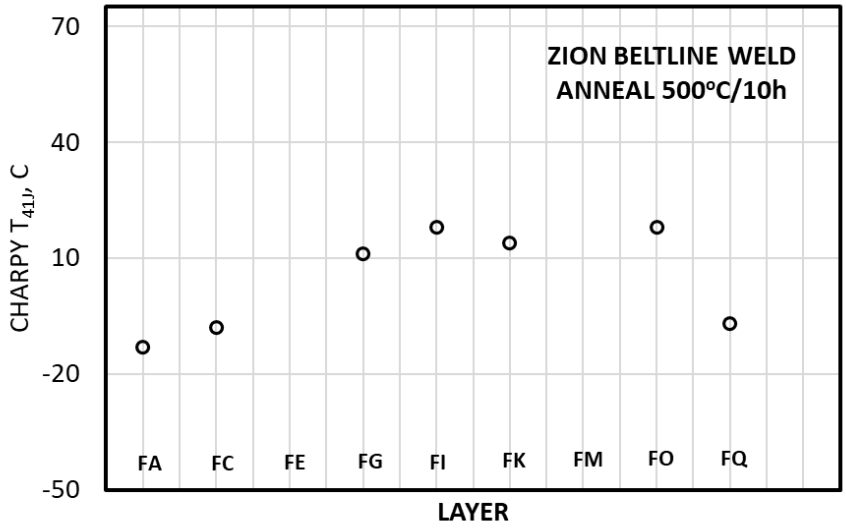

Figure 8. Distribution of the Charpy 41J transition temperature for Zion beltline weld specimens after post-rradiation annealing at 500°C for 10h.

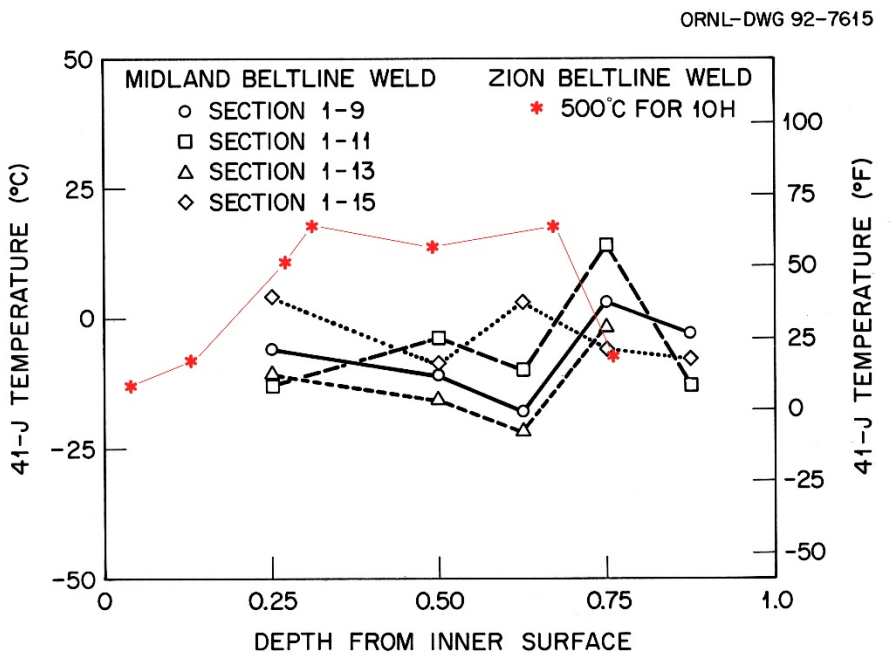

Figure 9. Charpy T_{41J} transition temperature of Midland unirradiated beltline weld and the annealed Zion beltline weld. Both welds are designated as WF-70.

Based on the transition temperatures obtained with the annealed specimens, the Charpy 41J transition temperature shift is shown in Fig. 10. It is clear that using the annealed data to account for the irradiation-induced change in the Charpy shift leads to results that are more consistent with expectations. This will be discussed further below in reference to Fig. 16.

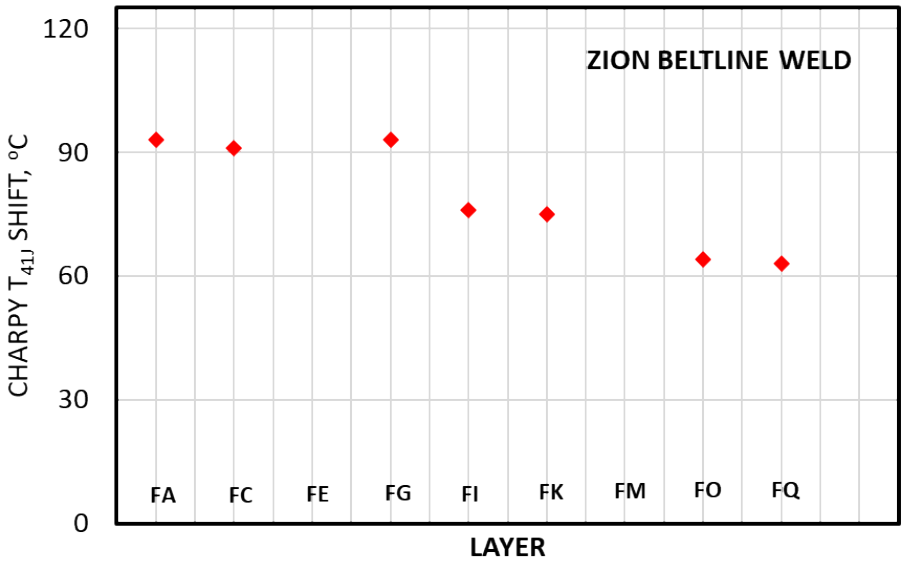

Figure 10. Shift of the Charpy transition temperature through the thickness of Zion RPV beltline weld. Unirradiated properties based on Charpy data from post-irradiation annealed specimens.

MODELING ASSESSMENT OF ZION DATA

Since the initial change in mechanical properties of the Zion beltline materials obtained using the surveillance weld as a basis did not follow the expected behavior as function of depth in the vessel, a previously developed computational model was used to investigate the potential reasons for this behavior. The development of the model and its application to RPV embrittlement was discussed in Refs. [14,15]. Briefly, the model simulates the radiation-induced evolution of point defect (vacancy and interstitial) clusters and copper-rich precipitates which give rise to hardening and embrittlement. The well-known reaction rate theory method is employed which permits the effects of parameters such as the neutron flux (atomic displacement rate) and irradiation temperature to be explicitly included. Relevant material parameters and the copper content are specified as input parameters.

As an example of the model behavior, Fig. 11 provides representative results from the model for matrix hardening as a function of displacement rate at 288°C at a total dose of 0.01 dpa, which is similar to the maximum dose on the Zion RPV materials. Material parameters used in the model to obtain the results of Fig. 11 are similar to those discussed in References 14 and 15. The values shown in the figure can be converted to yield strength change and Charpy shift using standard conversions as discussed in [14], but it seems more suitable to focus on the parameters calculated directly by the model for the purpose of this illustration. Values are shown for the three defect types mentioned above, along the total hardening based on the root sum-of-squares (RSS) of the individual components. The potential impact of a reduced displacement rate (neutron flux) as a function of depth into the RPV can be inferred from this

figure. For values typical of RPV materials, hardening from point defect clusters decreases and hardening from copper-rich precipitates increases as the displacement rate decreases. Because of the opposing effect of displacement rate on different types of defects, the total hardening can either increase or decrease with damage rate. The displacement rate at which the minimum in total hardening occurs will be a function of alloy composition and other material and irradiation parameters.

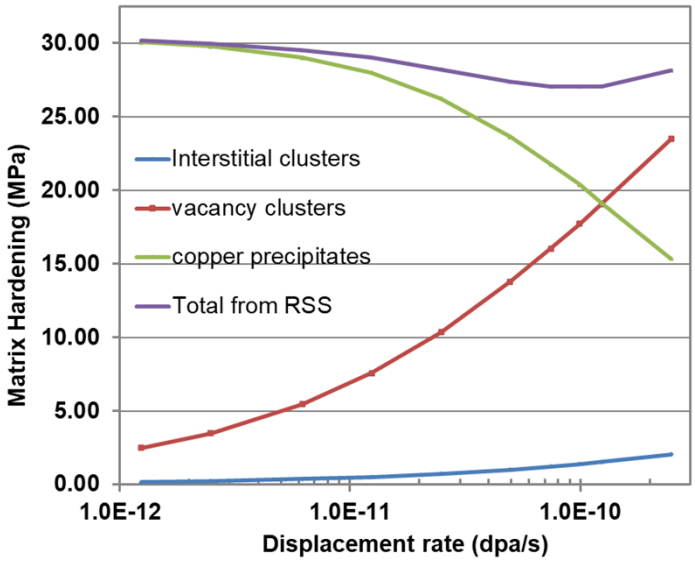

Figure 11. Predicted hardening for different microstructural defects for irradiation at 288°C to 0.01 dpa. Copper content is 0.3 atom-%, other parameters similar to those used in Ref. [15].

However, the results shown in Fig. 11 are for a constant total dose, which does not represent the through-thickness dose behavior obtained in an RPV. Fig. 12 shows the attenuation in dpa for an 8.8-inch (22,4 cm) thick RPV based on the exponential attenuation formula from Regulatory Guide 1.99/2 [4]. This is compared with the dpa values obtained from detailed transport calculations for a typical pressurized water reactor [16]. As pointed out previously [17], the dpa attenuation through the RPV is slower than what is predicted by the NRC exponential model. However, attenuation is relatively strong in both cases, and the relative attenuation is similar at the ¾-T position.

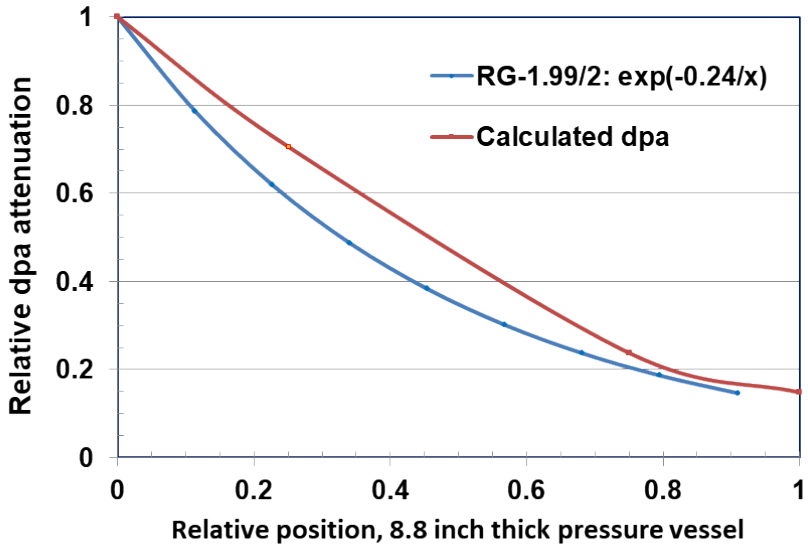

Figure 12. Relative attenuation of displacement rate through RPV. A comparison of the RG-1.99/2 [4] attenuation model with dpa obtained from neutron transport calculations [15].

It is important to point out that it is not proper to assume that the attenuation in mechanical properties will be the same as the attenuation in the primary damage term, i.e. the atomic displacement rate or fast fluence. This is another way of saying that mechanical property damage accumulation is not simply a linear function of radiation damage exposure. The difference is clear when comparing the results from Fig. 12 with those in Fig. 13. Although Fig. 12 indicates that total dose is reduced by about 80% at the ¾-T position, applying this reduction in the RG-1.99/2 embrittlement trend curve leads to ~40% of the predicted embrittlement at the RPV inner surface when the RG-1.99/2 attenuation model is used. As expected from Fig. 12, using the calculated dpa [16] leads to less attenuation. Application of the ASTM E900 embrittlement trend curve [5] with the same dose values indicates even less attenuation. In Figs 13 and 16, "exponential attenuation" refers to use of the RG-1.99/2 exponential attenuation model where the fast fluence at any depth x, $f(x) = f_{surf} e^{-0.24x}$. Here, f_{surf} is the fast fluence (E>1.0 MeV) at the inside surface of the RPV.

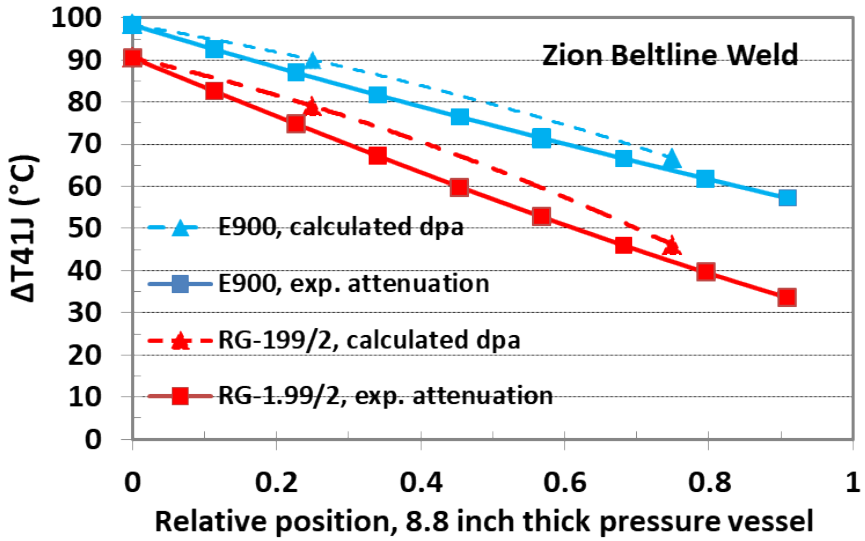

Figure 13. Attenuation of Charpy 41J transition temperature shift estimated for Zion beltline weld with different embrittlement trend curves and dpa attenuation models.

Although the predictions of such microstructural models are sensitive to the assumed material parameters, they are reasonably consistent with the experimentally based embrittlement trend curves. This is shown in Fig. 14 in which results of the RG-1.99/2 trend curve for the Zion RPV are compared with model predictions obtained using two alternate parameter sets. The case with the higher assumed copper precipitate density and matrix free surface energy leads to greater embrittlement near the inside surface and more rapid attenuation. Although the case with a lower precipitate density and surface energy predicts a lower maximum level of Charpy shift than RG-1.99/2, and the rate of attenuation is nearly the same as the Regulatory Guide. The cross-over in the two predicted curves at about 0.65-T is related to the displacement rate change and the balance between point defect hardening and precipitate hardening as discussed with respect to Fig. 11 above.

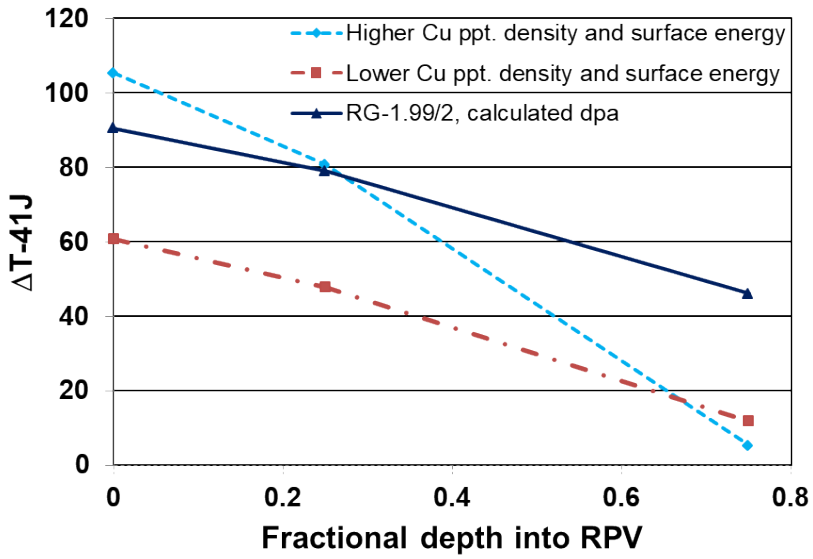

Figure 14. Comparison of Charpy 41J transition temperature shifts obtained for the Zion beltline weld using the microstructural model [15]and the RG-1.99/2 embrittlement model [4]. Calculated dpa values [16] were used for attenuation in the RG-1.99/2 model.

A variety of material and irradiation parameters were investigated using both the embrittlement trend curves and the microstructural models in an attempt to understand the behavior of the Zion beltline materials. For example, the copper and nickel contents of individual samples were used as opposed to the nominal average values (Cu=0.35, Ni=0.59 wt-%) to see their impact on the results obtained with the RG-1.99/2 trend curve. The results shown in Fig. 15 were obtained using the measured Cu and Ni concentrations listed in Table 3. Note that the lower copper values measured between about 0.25-T and 0.5-T [1] would lead to smaller Charpy shifts being predicted by RG-1.99/2 in the same region where the measured shifts are larger. If E900 was used rather than RG-199/2, the shift values obtained using local chemistries would be more similar to those with the nominal chemistry because E900 specifies a maximum effective copper concentration of 0.28 wt-%.

Table 3. Location-specific chemistries used in Figure 15.

RPV depth (t/T)	Cu (wt-%)	Ni (wt-%)
0.063	0.355	0.565
0.161	0.355	0.555
0.259	0.305	0.525
0.358	0.325	0.520
0.456	0.300	0.525
0.555	0.340	0.545
0.653	0.360	0.580
0.752	0.355	0.515
0.850	0.280	0.575

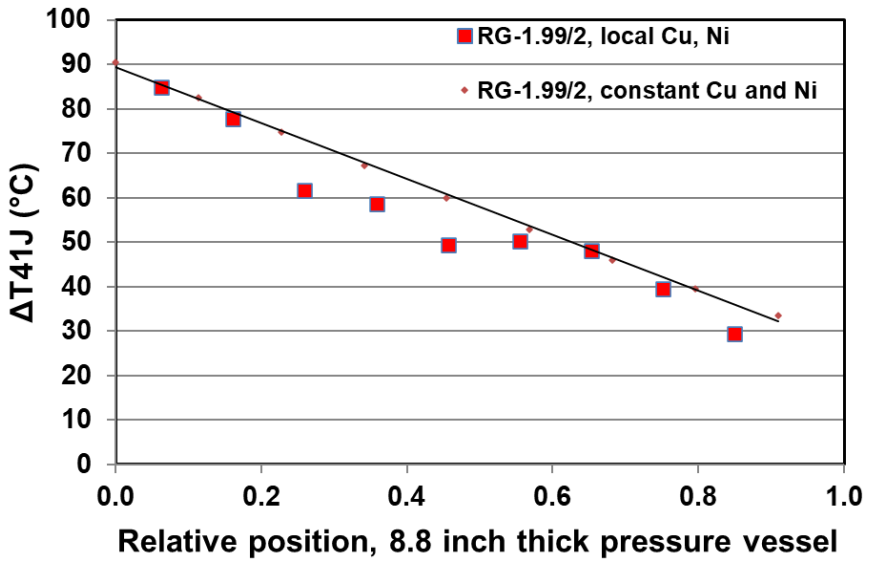

Figure 15. Comparison of Charpy shift estimated with RG-1.99/2 embrittlement trend curve using both local and nominal chemistry values.

The results of the analysis based on the computational model and standard embrittlement model failed to provide any insight into potential reasons for why the initially measured Charpy 41J transition temperature shifts (Fig. 7) deviated so significantly from the expected behavior. The simulations obtained using the microstructural model were broadly consistent with the embrittlement trend curves developed by the nuclear industry, and both were inconsistent with the Zion data summarized in Fig.7. However, using post-irradiation annealing to obtain what is believed to be a better approximation of the unirradiated properties yields reasonable agreement between the data and the ASTM E900 embrittlement correlation [5] as shown in Fig. 16. Note that although E900 predicts somewhat higher shifts for these

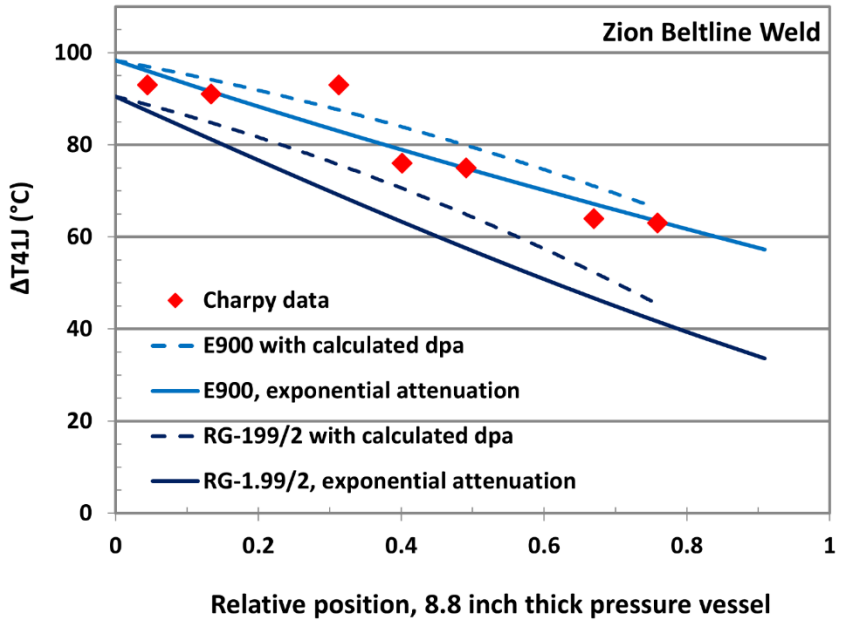

conditions than does RG-199/2, the relative attenuation trend observed is similar. These results emphasize the importance of having an accurate measurement of the unirradiated material properties in order to accurately determine the changes induced by radiation.

Figure 16. Comparison of Charpy 41J transition temperature shifts for Zion beltline weld with different embrittlement trend curves and dpa attenuation models.

DISCUSSION

As mentioned above, previous post-mortem examinations of damage attenuation in commercial RPVs, as well as data from specifically designed damage attenuation irradiation experiments, have shown significant deviations from simple attenuation models [6,7,10,11]. Although that data will not be revisited in any detail here, several examples will be shown to provide a comparison with the Zion results in Fig 16.

The first example is from the sampling of the Chooz A vessel in France. Fig. 5 in Ref. [18] is a plot the 56J transition temperature shift as a function of depth into the Chooz A RPV. The unirradiated curve in this figure was obtained based on the measured through-thickness profile of a shell forging (same grade and same manufacture) used in the qualification process of the Chooz A vessel and an unirradiated ¼-T transition temperature measurement from the Chooz A surveillance program. The data from Fig. 5 of Ref. [18] were digitized and replotted in Fig. 17 to show the transition temperature shift. The most notable similarity between the Zion data in Fig. 5a and the Chooz A data in Fig. 17 is the apparent increase in the shift between the ¼ and ½-T positions. Although damage attenuation in the Chooz A RPV is initially consistent with the RG-1.99/2 dpa-based attenuation, significantly less attenuation is observed beyond the ¼-T location. Although it should not have a significant impact on the results shown here, it should be pointed out that the specimens in the Chooz surveillance program were in the LT orientation, while the specimen machined from the irradiated Chooz RPV were in the TS orientation in order to avoid fluence variation along the notch root.

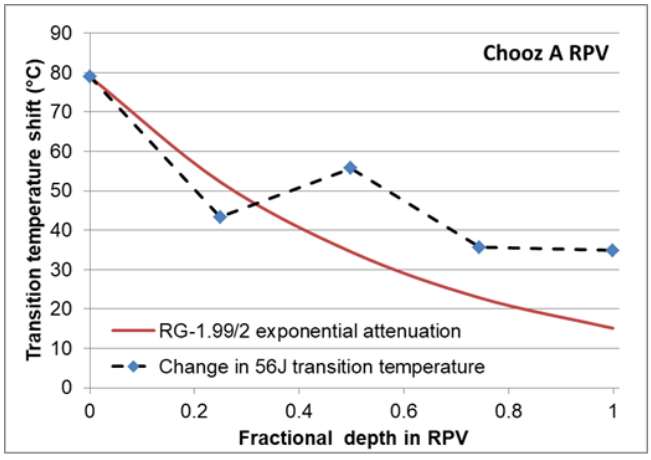

Figure 17. Transition Temperature Shift (56J) as a Function of Depth in Chooz A RPV [18].

A second example comes from the Gundremmingen Unit A RPV. An extensive post-irradiation testing program was carried out on both base and weld material. In some cases the through-thickness data was relatively well-behaved. However, data from one of the welds was more problematic. The results shown in Fig. 18 were obtained from Fig. 22 in Ref. [10]. As was done for the Chooz A data in Fig. 17, the measured transition temperatures for RPV and archive material were used to obtain the transition temperature shifts through the vessel. The results clearly deviate from the simple exponential attenuation function of RG-1.99/2. Most of the unexpected behavior is a result of the variation in the through-thickness properties of the unirradiated archive material.

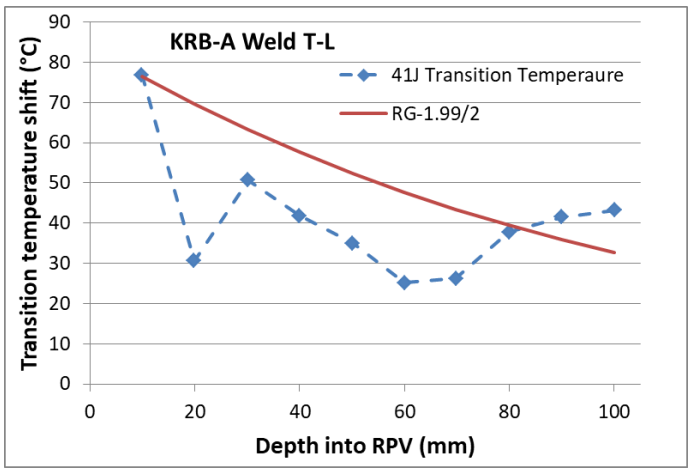

Figure 18. Transition Temperature Shift (Δ41J) as a Function of Depth in Gundremmingen RPV [9].

A third example is taken from the IAEA-Czech NRI attenuation experiment [11]. Depending on the specimen location in the experiment, the JRQ reference plate material was irradiated to fluences between about 5.4×10^{23} and 3.0×10^{22} n/m^2. The Master Curve T_0 data from Fig.8 in Ref. [11] have been replotted as shown in Fig. 19. The data point at about 50 mm into the simulated RPV may be anomalous, showing greater embrittlement than the two higher fluence points, and it should be pointed out that the corresponding Charpy data did not exhibit this behavior. However, it is not clear which, if any, of these data are anomalous. As in Figs. 17 and 18, the data are compared to the RG-1.99/2 attenuation function. Here the attenuation curve was fixed in two alternate locations for purposes of comparison. The solid red line is fixed to the highest fluence, "near surface," data point, while the dashed red line is fixed using the highest shift data point at 50 mm. The lower fluence (farther from the inside surface) data points are more closely tracked by the dashed line, which suggests that either the damage attenuation is much slower than

the attenuation function, or perhaps the actual shift at the two highest fluence points is higher than the measurements indicated.

As mentioned above, there is some similarity between this data and the Zion data shown in Fig. 7, viz. the shift data is not monotonic with respect to the depth. Taken at face value, the shift initially increases and then decreases at a rate consistent with RG-1.99/2 [14]. The highest shift value is roughly at an equivalent RPV ¼-T position. In the case of the Zion data shown in Figs. 10 and 16, using data from post-irradiation annealed specimens (Fig. 8) to provide the properties of the unirradiated material appears to make the Charpy shift data consistent with standard embrittlement correlations (Fig. 16). The renormalized attenuation curve in Fig. 19 suggests that the shift values obtained at the two highest fluence points may be higher than the initial measurements indicated. An obvious explanation would be that the unirradiated T_{41J} values were lower. In both cases, the discrepancies highlight the need for accurate unirradiated values.

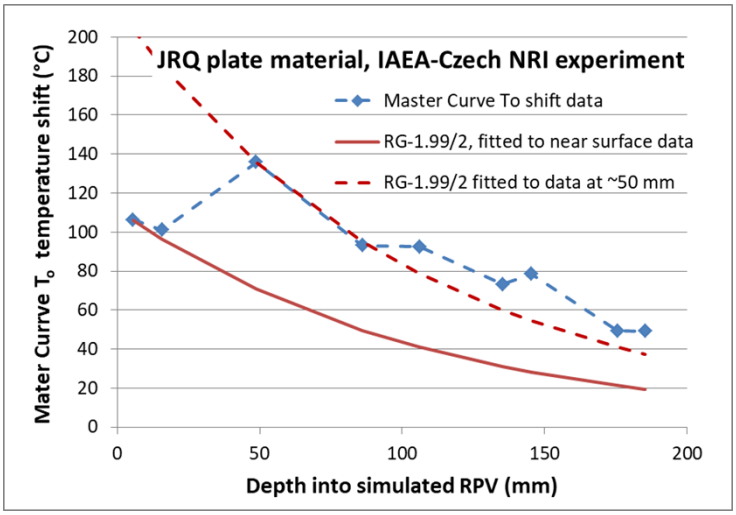

Figure 19. Master curve, T_0, temperature shift of JRQ plate material in IAEA-Czech NRI attenuation experiment [11].

A forth illustration is provided by a comparison between the behavior of the circumferential and axial beltline welds of the Barsebäck 2 reactor in Sweden [19]. The ¼-T location of this boiling water reactor pressure vessel was evaluated for these welds after the reactor was decommissioned. Because it was a BWR, the maximum fluence was relatively low; the peak fluence at the inner surface for the axial weld was ~7.9×10^{21} n/m^2 and ~2.9×10^{20} n/m^2 for the circumferential weld. At the ¼-T location, the shift measured for the circumferential weld was in good agreement with the prediction based on the surveillance data (~5°C) while the axial weld was substantially tougher than predicted at this location. The predicted shift was ~40°C greater than the measured shift for this weld. The authors of Ref. [19] attributed these differences to variations in post-weld heat treatments.

A final example comes from the examination of a weld from the RPV of the decommissioned Greifswald nuclear power plant [20]. This presents data from a different class of steel because it was one of the first generation of Russian-type WWER-440/V-230 reactors. The reactor operated for 11 years, and the fluence (E>0.5 MeV) of weld specimens cut from the vessel varied between ~9.2×10^{18} n/cm^2 near the outer surface and ~4.1×10^{19} n./cm^2 near the inner surface. The Russian weld designation was 10KhMFT, which had higher chromium and vanadium levels and a lower nickel level than the common western steels such as A533B or A508. Post-irradiation examination showed that the welding procedure used had led to dramatic variations in composition as a function of depth into the pressure vessel. The weld root was near the ¼-T location, and the copper and phosphorus concentrations were reduced by a factor of two in this region. Somewhat smaller but still significant variations of C, Cr, Mn, and V were also observed in this region.

Given the observed spatial variation of the concentration of critical embrittling elements such as Cu and P, it is not surprising that the through-thickness mechanical properties did not show a systematic effect of the fluence attenuation through the RPV. The observed Charpy transition temperature at 47J decreased from ~75°C near the surface to ~35°C at the ¼-T location, then increased to ~125°C between 0.4 and 0.8-T before dropping again to ~90°C near the outer surface. The authors concluded "...the predicted irradiation-induced ductile-to-brittle transition temperature shift was not confirmed by the values measured on specimens from the multilayer beltline welding seam 0.1.4 and forged base metal ring 0.3.1." This was attributed primarily to the effect of the weld root, variations in the weld bead structure, and significant compositional inhomogeneity.

CONCLUSIONS

As discussed above, the data from studies of damage attenuation through an irradiated RPV are complex and largely inconclusive with respect to the apparent reduction of embrittlement with fluence [6-12, 18-20]. Results from a given post-mortem RPV examination or a given irradiation experiment reveal unexplained variations between materials. Plausible explanations include compositional differences, variations in heat treatments, different welding procedures, and datapoints that are "outliers" for unknown reasons.

On the first examination, the data from the Zion RPV seemed to be similarly inconsistent with expectations. However, the use of post-irradiation annealing at 500°C with the goal of recovering the radiation-induced damage clearly appears to produce reasonable agreement with standard industry embrittlement correlations as shown in Fig. 16. Together with the explanations offered for previous unexpected data on damage attenuation observed on some other RPVs as discussed above, it seems clear that further research is needed to make it possible to confidently predict the mechanical properties as a

function of depth into the RPV. In particular, an accurate assessment of the unirradiated through-thickness properties is required.

Acknowledgments

This research was sponsored by the U.S. Department of Energy, Office of Nuclear Energy, Light Water Reactor Sustainability Program Materials Research Pathway under contract DE-AC05-00OR22725 with UT-Battelle, LLC / Oak Ridge National Laboratory. The authors wish to thank Xiang (Frank) Chen and Igor Remec who reviewed the manuscript. We also would like to thank Bill Server for discussion and comments on the manuscript. Continuous support from Xiang (Frank) Chen and Thomas Rosseel, the current and former Pathway Leads of the Long-Term Performance Pathway of the Light Water Reactor Sustainability Program, is highly appreciated.

REFERENCES

1. Rosseel, T.M.; Sokolov, M.A.; Chen, X.; Nanstad, R.K., Harvesting Reactor Pressure Vessel Beltline Material from the Decommissioned Zion Nuclear Power Plant Unit 1. Metals 2025, 15, 634. https://doi.org/10.3390/met15060634
2. Rosseel, T. M., Sokolov, M. A., Chen, X., Nanstad, R. K., "Report on the Completion of the Machining of Zion Unit 1 Reactor Pressure Vessel Blocks into Mechanical and Microstructural Test Specimens and Chemical Analysis Coupons," ORNL/TM-2018/861, May 2018.
3. Stelzman, W.J, Berggren, R.G., and Jones, T.N., "ORNL Characterization of Heavy-Section Steel Technology Program Plates 01, 02, and 03," ORNL/TM-9491, NUREG/CR-4092, April 1985.
4. "Radiation Embrittlement of Reactor Vessel Materials," Regulatory Guide 1.99, Revision 2, U.S. Nuclear Regulatory Commission, May 1988, available from the U.S. National Technical Information Service, Springfield, VA.
5. ASTM E900-21, Standard Guide for Predicting Radiation-Induced Transition Temperature Shift in Reactor Vessel Materials, ASTM International, West Conshohocken, PA.
6. English, C., and Server, W. L., "Attenuation in U.S. RPV Steels," EPRI Materials Reliability Program (MRP-56), Electric Power Research Institute, Palo Alto, CA, June 2002.
7. English, C., Server, W. L., and Rosinski, S. T., "Critical Review of Through-Wall Attenuation of Mechanical Properties in RPV Steels," presented at the 21st International Symposium on the Effects of Radiation on Materials, Journal of ASTM International 1 (2004) 23 pages, https://doi.org/10.1520/JAI11246.
8. Nanstad, R. K., McCabe, D. E., and Swain, R. L., "Evaluation of Variability in Material Properties and Chemical Composition for Midland Reactor Weld WF- 70," Effects of Radiation on Materials, STP 1325, R. K. Nanstad, M. L. Hamilton, F. A. Garner, and A. S. Kumar, Eds., American Society for Testing and Materials, West Conshohocken, PA, 1999, pp. 125-156.
9. Reference Manual on the IAEA JRQ Correlation Monitor Steel for Irradiation Damage Studies, IAEA-TECDOC-1230, Int. Atomic Energy Agency, Vienna, July 2001.
10. Kussmaul, K, Föhl, J., and Weissenberg, T., "Investigation of Materials from a Decommissioned Reactor Pressure Vessel—A Contribution to the Understanding of Irradiation Embrittlement," Effects of Radiation on Materials: 14th International Symposium (Volume II), ASTM STP 1046, N. H. Packan, R. E. Stoller, and A. S. Kumar, Eds., ASTM International, West Conshohocken, PA, 1990, pp. 80-104.
11. Server, W. L., Brumovský, M., Kytka, M., Soneda, N., and Spanner, J. C., "Further Results on Attenuation of Neutron Embrittlement Effects in a Simulated RPV Wall," Journal of ASTM International 7 (2010) 11 pages, https://doi.org/10.1520/JAI102070.
12. Sokolov, M. A. and Stoller, R. E., "Analysis of Attenuation Effects Based on Results from Zion Beltline Reactor Pressure Vessel," Light Water Reactor Sustainability Program, Materials Research Pathway Milestone Report: M3LW-24OR0402015, Oak Ridge National Laboratory, September 2024.
13. Eason, E.D., Wright, J.E., Nelson, E.E., Odette, G.R., and Mader, E.V., "Embrittlement recovery due to annealing of reactor pressure vessel steels," Nuclear Engineering and Design 179 (1998) 257–265.
14. Stoller, R.E. "The Influence of Damage Rate and Irradiation Temperature on Radiation-Induced Embrittlement in Pressure Vessel Steels," Effects of Radiation on Materials, 16th International

Symposium, ASTM STP 1175, A. S. Kumar, D. S. Gelles, R. K. Nanstad, and E. A. Little, Eds., American Society of Testing and Materials, Philadelphia, 1993, 394-426.

15. Stoller, R.E. “Pressure Vessel Embrittlement Predictions Based on a Composite Model of Copper Precipitation and Point Defect Clustering,” Effects of Radiation on Materials, D. S. Gelles, R. K. Nanstad, A. S. Kumar, and E. A. Little, Eds., ASTM STP 1270, American Society of Testing and Materials, Philadelphia, 1996, pp. 25-59.
16. Albert, T.E., Gritzner, M.L., Simmons, G.L., and Straker, E.A. “PWR and BWR Radiation Environments for Radiation Damage Studies, “EPRI NP-152, Electric Power Research Institute, Palo Alto, CA, September 1977.
17. Stoller, R.E., and Greenwood, L.R., “An Evaluation of Through-Thickness Changes in Primary Damage Production in Commercial Reactor Pressure Vessels,” Effects of Radiation on Materials, S. T. Rosinski, M. L. Grossbeck, T. R. Allen, and A. S. Kumar, Eds., ASTM STP 1405, American Society of Testing and Materials, West Conshohocken, PA, 2001, pp. 204-217.
18. Brillaud, C., Grandjean, Y., Saillet, S.,"Vessel Investigation program of CHOOZ A PWR Reactor After Shutdown," Effect of Radiation on Materials : 20th International Symposium, ASTM STP 1405, S. T. Rosinski, M. L. Grossbeck, T. R. Allen, and A. S. Kumar, Eds., American Society for Testing and Materials, West Conshohocken, PA, 2002.
19. Lindqvist, S., Norrgård, A., Arffman, P., Hytönen, N., Lydman, J., Efsing, P., Suman, S., and Nevasmaa, P., “Mechanical Behavior of High-Ni/High-Mn Barsebäck 2 Reactor Pressure Welds after 28 Years of Operation,” J. Nucl. Mater. 581 (2023) 154447, https://doi.org/10.1016/j.jnucmat.2023.154447.
20. Viehrig, Hans-Werner, Altstadt, Eberhard, Houska, Mario, and Valo, Matti, “Validation of Surveillance Concepts and Trend Curves by the Investigation of Decommissioned Reactor Pressure Vessels,” International Review of Nuclear Reactor Pressure Vessel Surveillance Programs, ASTM STP1603, W. L. Server and M. Brumovsky, Eds., ASTM International, West Conshohocken, PA, 2018, pp. 457–483, http://dx.doi.org/10.1520/STP160320160127.